Electronic Supplementary Material (ESI) for New Journal of Chemistry.

Development of Z-scheme bimetallic tungstate-supported nitrogen deficient g-C_3N_4 heterojunction for the treatment of refractory pharmaceutical pollutants

H. Leelavathi [a], R. Muralidharan [b], N. Abirami [a], R. Arulmozhi [a*]
[a] Department of Chemistry, SRM Institute of Science and Technology, Kattankulathur, Chengalpattu-603 203, Tamil Nadu, India.
[b] Department of Physics, Saveetha School of Engineering, Saveetha Institute of Medical and Technical Sciences, Thandalam, Chennai-602 105, Tamil Nadu, India.
*arulmozr@srmist.edu.in

3. Results and Discussion

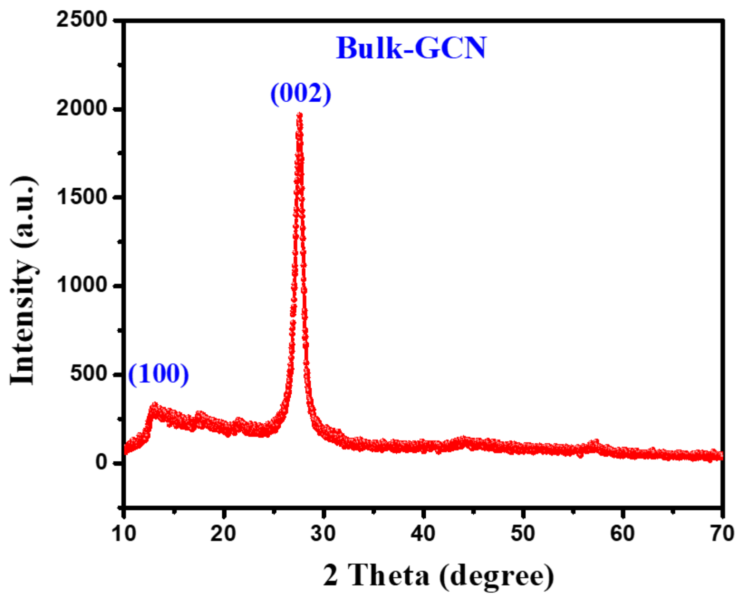

Fig. S1 PXRD spectrum of bulk-GCN.

Table S1 Lattice parameters and particle sizes of the fabricated samples.

Sample	a (Å)	b (Å)	c (Å)	Phase	Crystallite Size (nm)
NCW	4.67	5.69	4.94	Monoclinic	25.06
NCW/ND-GCN	4.70	5.71	4.96	Monoclinic	14.90
CZW	4.65	5.69	4.98	Monoclinic	35.19
CZW/ND-GCN	4.69	5.72	4.95	Monoclinic	27.16

Table S2 Covalent bond distribution of N 1s binding energy of ND-GCN and bare-GCN.

Binding Energy	(C=N-C)	(N-H)	($C-NH_2$)
ND-GCN	398.87 eV	400.01 eV	401.38 eV
	58.78 %	31.65 %	9.57 %
bare-GCN	398.6 eV	399.5 eV	401.1 eV
	51.09 %	39.77 %	9.14%

Table S3 SEM-EDX elemental analysis of bulk-GCN and ND-GCN.

Name of the Sample	Element	At (%)	Atomic ratio of C/N
bulk-GCN	C	40.09	0.67
	N	59.91	
ND-GCN	C	47.67	0.91
	N	52.33	

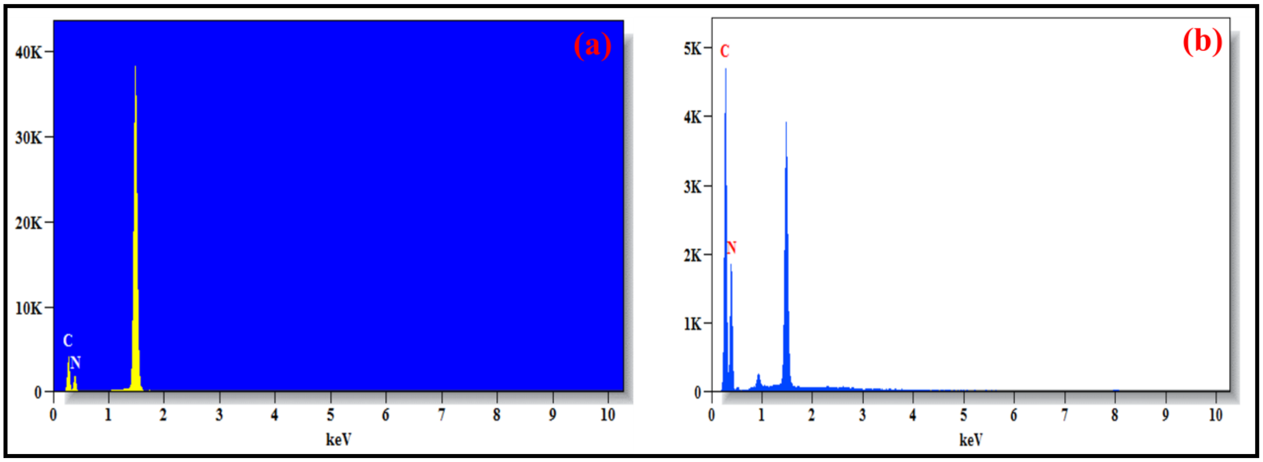

Fig. S2 Energy dispersive spectra of (a) bulk-GCN; and (b) ND-GCN.

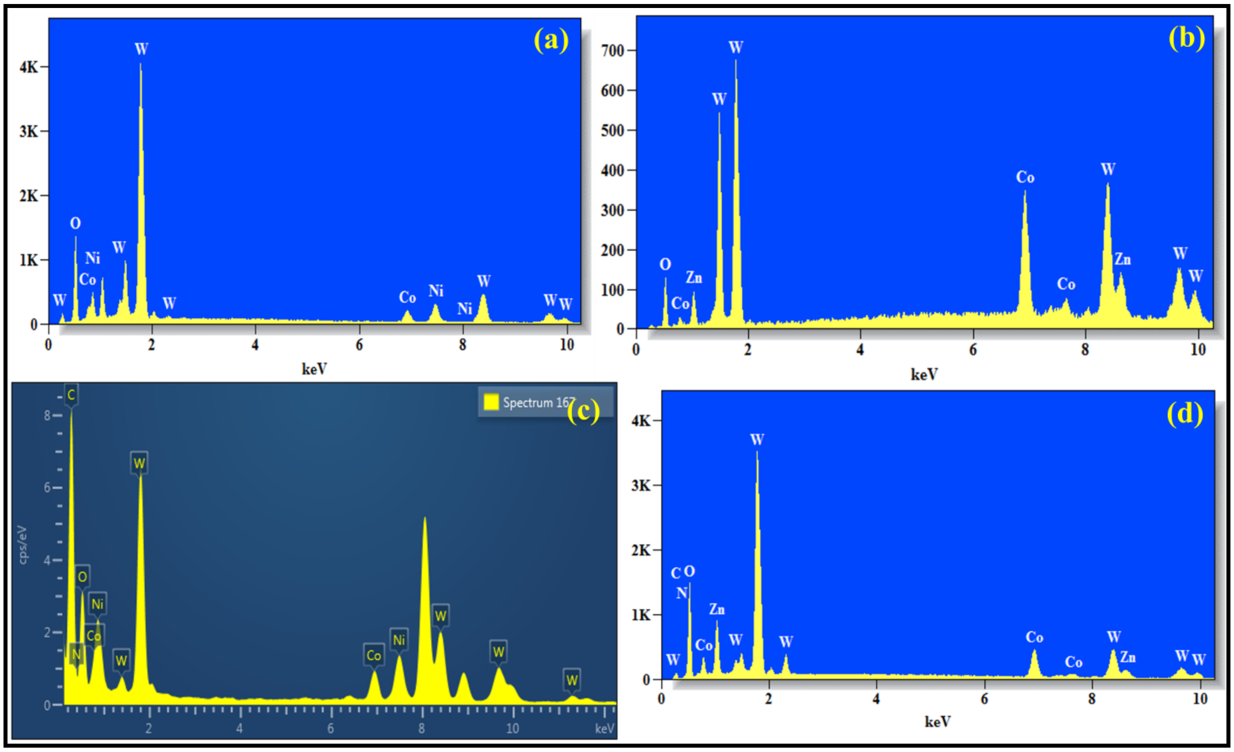

Fig. S3 Energy dispersive spectra of (a) NCW; (b) CZW; (c) NCW/ND-GCN; and (d) CZW/ND-GCN nanocomposite.

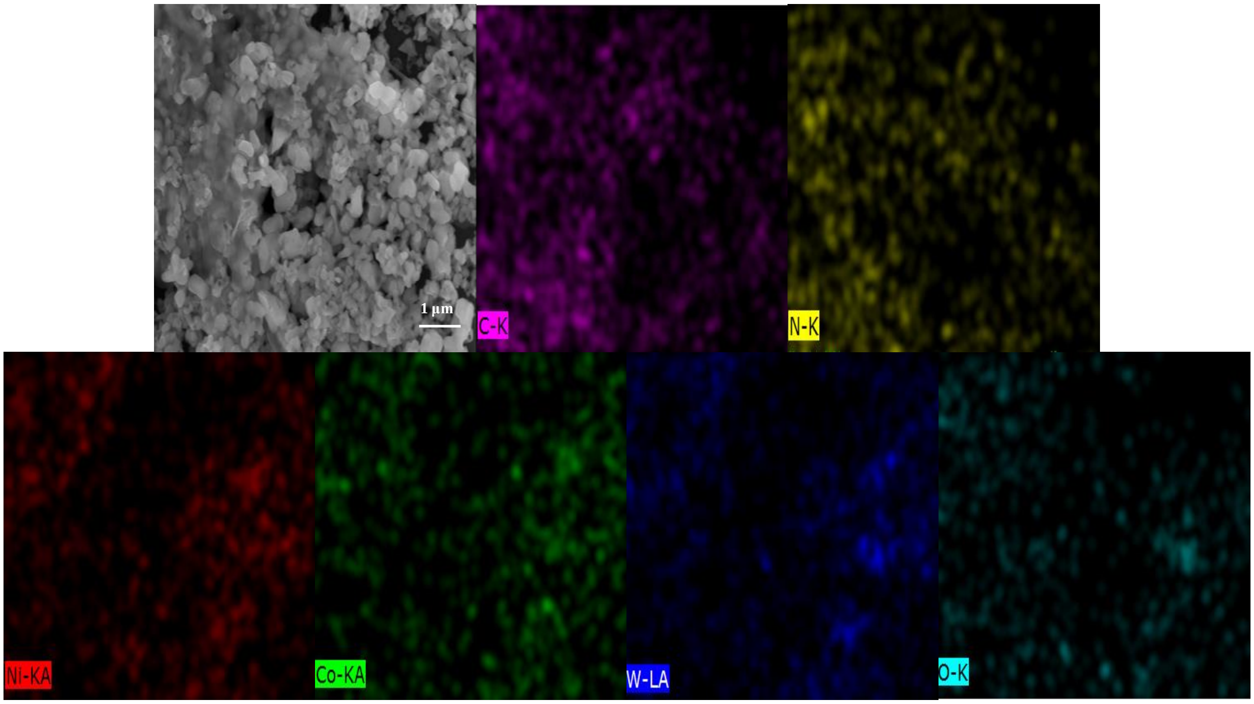

Fig. S4 SEM-EDX elemental mapping of NCW/ND-GCN nanocomposite.

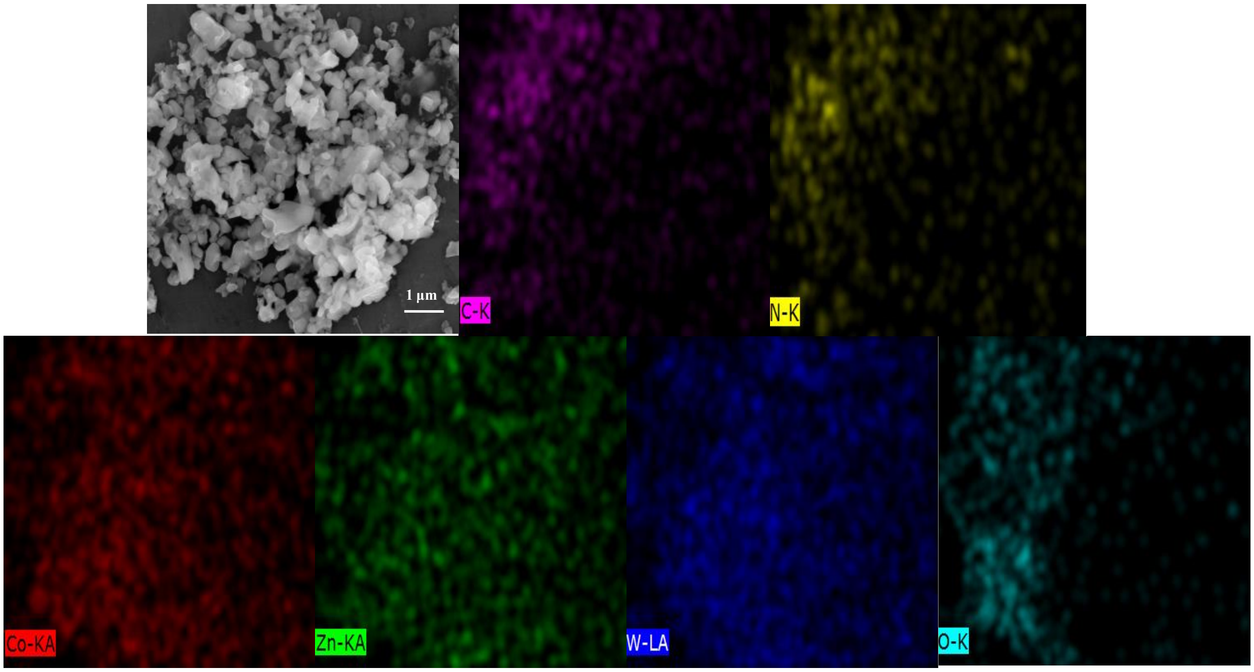

Fig. S5 SEM-EDX elemental mapping of CZW/ND-GCN nanocomposite.

Table S4 The CB and VB edge potentials of fabricated samples estimated using the Mulliken electronegativity concept and Mott Schottky studies.

Concept	Conduction Band (E_{CB})			Valance Band (E_{VB})		
	ND-GCN	**NCW**	**CZW**	**ND-GCN**	**NCW**	**CZW**
Mulliken electronegativity	-1.17 eV	+0.35 eV	+0.41 eV	+1.63 eV	+2.58 eV	+2.56 eV
Mott Schottky Study	-1.16 eV	+0.29 eV	+0.39 eV	+1.64 eV	+2.52 eV	+2.54 eV

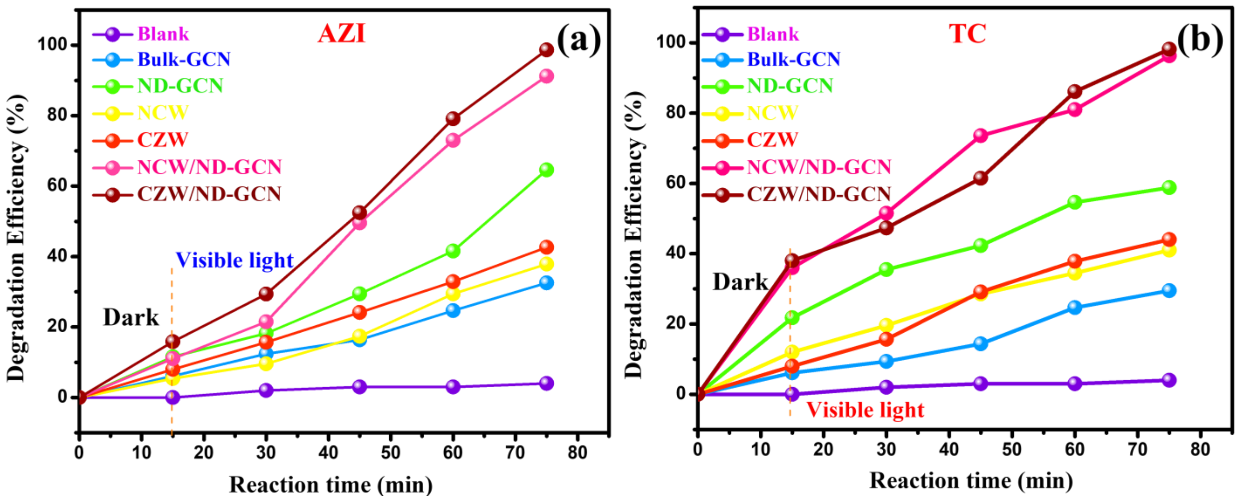

Fig. S6 The dye degradation rate (%) of blank, bulk-GCN, ND-GCN, NCW, CZW, NCW/ND-GCN and CZW/ND-GCN nanocomposite at various irradiation times (min) over (a) AZI; b) TC antibiotic drugs.

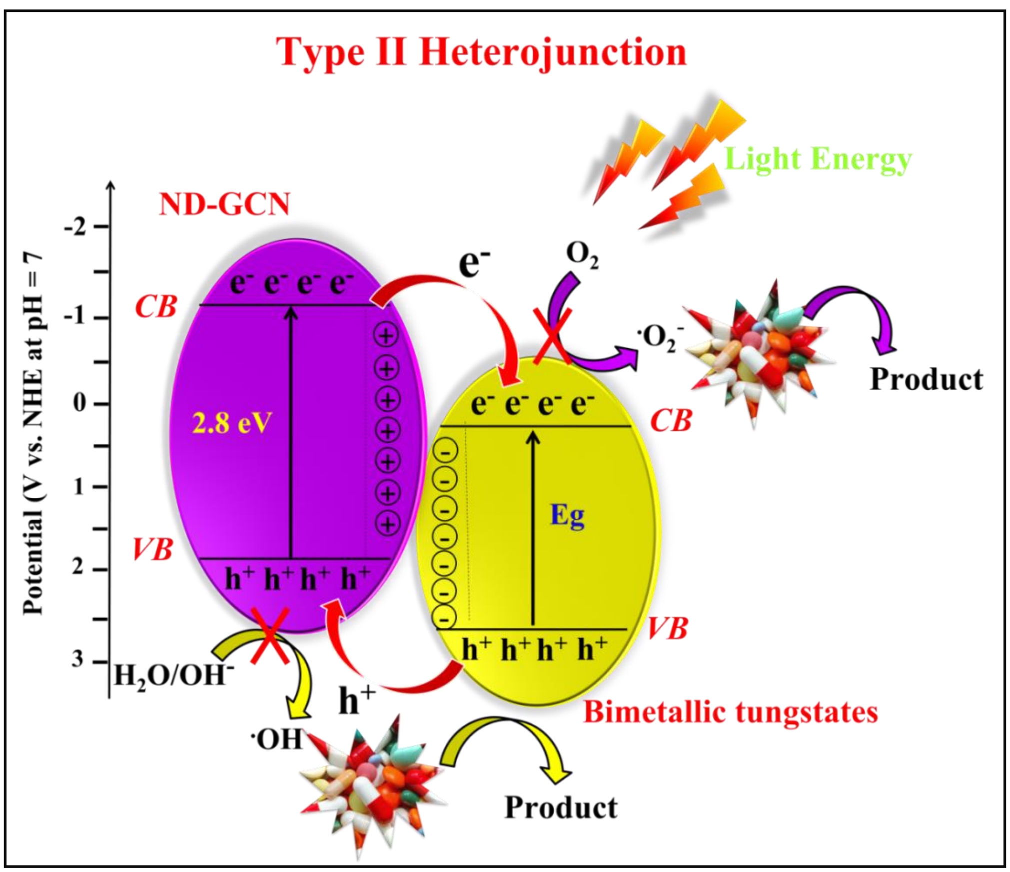

Scheme S1 Deciphering the impossibility of type-II heterojunction formation.

Table S5 Correlation of photocatalytic antibiotic degradation efficiency of current work with the several recently published bare tungstates and ND-GCN-based nanomaterials.

Name of the Photocatalyst	Weight of Catalyst	Concentration of organic pollutant	Source of visible light	Irradiation time (min)	Efficiency of degradation (%)
$CuZnWO_4$/rGO [58]	50 mg	100 mg L^{-1}	300 W Xe lamp	80 min	73 %
Ni-$CoWO_4$ [59]	50 mg	5 ppm	300 W Xe lamp	150 min	48.72 %
$CuWO_4$ [60]	0.05 g	15 ppm	Fluorescent lamp-32 W	240 min	80 %
ND-g-C_3N_4 [61]	100 mg	30 mg L^{-1}	300 W Xe lamp	90 min	80.61 %
ND-g-C_3N_4 [62]	50 mg	10 mg L^{-1}	300 W Metal halide lamp	300 min	100 %
This work (CZW/ND-GCN)	50 mg	70 ml (Pharma effluent)	300 W Xe lamp, (Visible)	90 min	97.84 %